

Mechanical Effects of Biogenic Nitrogen Gas Bubbles in Soils

Veronica Rebata-Landa¹ and J. Carlos Santamarina, M.ASCE²

Abstract: The fluid bulk stiffness of a soil is very sensitive to the presence of gas, and a small volume of bubbles can significantly affect the pore pressure response to loading, including Skempton's B parameter, P -wave velocity, and liquefaction resistance. Biologically mediated processes can lead to the production of gases in soils; nitrogen is particularly advantageous because it is not a greenhouse gas, it is not combustible, and it has low solubility in water. Sands, silts, and clayey sands inoculated with *Paracoccus denitrificans* were monitored to assess the effects of nutrient availability, fines content, and pressure-diffusion on the evolution of nitrogen gas generation and bulk stiffness. Results show clear evidence of biogas bubble formation, earlier gas generation and entrapment in specimens with higher fines content, and a strong correlation between biogas volume and P -wave velocity. The volume of gas is correlated with specific surface, suggesting that biogas bubble formation develops as heterogeneous nucleation and that it is directly linked to the availability of nucleation sites on mineral surfaces, which in turn also affect the degree of attainable supersaturation. Results support the viability of biogenic gas generation as a tool to increase the liquefaction resistance of soils subjected to cyclic loading. DOI: 10.1061/(ASCE)GT.1943-5606.0000571. © 2012 American Society of Civil Engineers.

CE Database subject headings: Stiffness; Soil gas; Bubbles; Velocity; Pore pressure; Nitrogen.

Author keywords: Bulk Stiffness; Undrained strength; Biogenic gas; Gas bubbles; P -wave velocity.

Introduction

The undrained strength and the liquefaction resistance can be enhanced by reducing the contractive tendency of soils (i.e., through densification), by increasing their threshold strain [e.g., by injecting foams or plastic fines (Gallagher and Mitchell 2002)] Per MP's feedback, by increasing their small strain stiffness [i.e., light cementation to prevent early pore pressure generation (Ismail et al. 2002)], or by decreasing their pore fluid bulk stiffness (Yang et al. 2004; Yegian et al. 2007). The field application of these alternatives can be restricted by the presence of nearby buildings, high cost, uncertainty of execution, or possible environmental implications.

The fluid bulk stiffness is very sensitive to the presence of gas, and a small volume of bubbles can significantly affect the pore pressure response to loading including the value of Skempton's B parameter, P -wave velocity, and liquefaction resistance (Chaney 1978; Fourie et al. 2001; Ishihara et al. 1998; Kokusho 2000; Tamura et al. 2002; Yoshimi et al. 1989; Yegian et al. 2007). Pore fluid softening by gas injection is limited by the percolation of air bubbles along preferential paths formed by interconnected large pore throats, thus failing to create a homogeneous distribution of small bubbles. Conversely, methods that cause a relatively homogeneous distribution of air bubbles in the pore fluid, such as gas generation by electrolysis (Yegian et al. 2007), appear effective in reducing the liquefaction potential of soils.

Gas bubbles may also accumulate in otherwise saturated soil matrices through gas dissolution and air trapping during infiltration and/or rapid water table rise (Constantz et al. 1988; Fayer and Hillel 1986) or in situ anaerobic microbial respiration (Buttler et al. 1991; Dinel et al. 1988). Previous studies on biogenic gas bubbles in soils are mainly related to the effect of bubbles on compressibility and undrained strength of shallow sediments containing relatively large gas-filled cavities surrounded by a matrix of saturated soil (Sills and Gonzalez, 2001; Sills et al. 1991). The influence of relatively small biogenic gas bubbles on the undrained response of sediments and their potential effects in liquefaction resistance and P -wave velocity requires further research.

This study reviews known bacterial metabolisms that generate gas as a by-product, conduct an experimental study to improve the understanding of the process of biogenic gas generation in soils, and analyze the data using poroelastic models that capture the influence of gas bubbles on P -wave velocity and Skempton's B parameter.

Review of Biogenic Gas Bubbles

Biogenic Gas

Biologically mediated processes can lead to the production of gases in porous media (Adams et al. 1990; Soares et al. 1988; Wheeler 1988). Table 1 summarizes the conditions and species involved in biogenic gas generation in previous studies reported in the literature. Gas production tends to mimic bacteria population growth rates, and therefore can be controlled by limiting bacterial activity through nutrient availability, and by environmental conditions such as temperature, among other factors (Sills and Gonzalez 2001). Pore scale geometric limitations also apply (Rebata-Landa and Santamarina 2006).

The most common biogenic gases found in near-surface soils are CO_2 , H_2 , CH_4 , and N_2 . Carbon dioxide (CO_2) has high

¹Consultant, 9100 Westheimer Rd. Apt. 324, Houston, TX 77063.

²Civil & Environmental Engineering, Georgia Institute of Technology, 790 Atlantic Drive, Atlanta, GA 30332 (corresponding author). E-mail: jcs@gatech.edu

Note. This manuscript was submitted on January 30, 2007; approved on May 23, 2011; published online on January 17, 2012. Discussion period open until July 1, 2012; separate discussions must be submitted for individual papers. This paper is part of the *Journal of Geotechnical and Geoenvironmental Engineering*, Vol. 138, No. 2, February 1, 2012. ©ASCE, ISSN 1090-0241/2012/2-128-137/\$25.00.

Table 1. Previous Studies on Biogenic Gas Generation

Species	Remarks	Gases	Reference
Indigenous bacteria from two mine soils in east Texas	NO ₃₋ added; no NO ₃₋ added; NO ₃₋ + H ₂ O↓ added	N ₂ O, N ₂	Johns et al. 2004
Indigenous bacteria from interstitial waters of sulfate-depleted marine sediments	After sulfate depletion Rate of ~ 13 μmole/liter/day	CH ₄	Martens and Berner 1974
Indigenous bacteria from a Brookston loam	NO ₃₋ added	N ₂ O, N ₂	Firestone et al. 1980
<i>Methanobacterium thermoautotrophicum</i>	Methane production started after 1 h lag and ceased after 5 h	CH ₄ , H ₂	Daniels et al. 1980
Indigenous bacteria from soils used for tomato plants	After a lag phase of ~ 20 h, gas was produced for 75 h	H ₂	Logan et al. 2002
Mixed anaerobic bacteria	Gas production inversely proportional to SRT. Total gas production ranged from 4 to 10 L/day	CH ₄ , H ₂	Nakamura et al. 1993
<i>Clostridium acetobutylicum</i>	Vigorous gas production	CO ₂ , H ₂	Behlulgil and Mehmetoglu 2002
Indigenous bacteria from soil at an experimental site	Maximum gas production started after 71 h	N ₂ O, N ₂	Cardenas et al. 2003
Mixed denitrifying bacteria	Nitrogen gas (N ₂) was present almost entirely in the gas phase	N ₂ O, N ₂ , CO ₂	Chung and Chung 2000
Indigenous bacteria from an estuarine clayey silt	Gas produced after 21 days and held in the sediment bed for the next 17 days	CH ₄ , CO ₂	Sills and Gonzalez 2001
Indigenous bacteria from a wood compost bed medium	NO _x removal (and presumed N ₂ production) was rapidly performed in batch studies	N ₂ , N ₂ O	Barnes et al. 1995
Indigenous bacteria from a fluvic hypercalcaric cambisol	Ratio N ₂ O/(N ₂ O + N ₂) was around 0.54 in all cases	N ₂ O, N ₂ , CO ₂	Cannavo et al. 2004

solubility in water, causing low residency time; methane (CH₄) is a greenhouse gas; and both methane and hydrogen (H₂) are combustible. By contrast, nitrogen gas (N₂) presents several advantages within the scope of this investigation: it is neither explosive nor a greenhouse gas; and its solubility in water is very low (Table 2), so less gas is needed to produce bubbles and the bubbles will remain undissolved for longer periods of time.

Nitrate Reduction and Respiratory Denitrification in Soils

Nitrate can be reduced in the environment through the direct path of ammonification in which the product is ammonia; or it can take the indirect path of respiratory denitrification, in which case the products may be nitric oxide, nitrous oxide, Add serial comma.

and nitrogen gas; the two paths are shown in Fig. 1. The relative contribution of denitrification and nitrate ammonification is a function of the carbon-to-nitrate ratio (Tiedje et al. 1982). Although denitrification dominates in environments rich in nitrate but relatively deficient in electron donors, ammonification is largely favorable in electron-rich environments where only low concentrations of nitrate are available (Cole and Brown 1980; Forsythe et al. 1988).

In respiratory denitrification, nitrate is reduced to dinitrogen through a battery of reactions catalyzed by specific enzymes, as indicated in Fig. 1. Pathway NO₃₋ NO₂₋ NH₄₊ corresponds to nitrate/nitrite ammonification, while NO₃₋ NO₂₋ NO₋ N₂O N₂ corresponds to respiratory denitrification (data from Mohan et al. 2004; Moura and Moura 2001; Richardson et al. 2001; Simon 2002).

Table 2. Common Metabolisms that Generate Gas as a By-Product

Metabolism	Biomediated reaction	Generated gas	Henry's constant k_H M/atm ^a
Aerobic respiration	CH ₂ O + O ₂ → CO ₂ + H ₂ O	Carbon dioxide CO ₂	3.4 × 10 ⁻²
Fermentation	CH ₂ O → 0.333CH ₃ COOH + 0.333CO ₂ + 0.667H ₂	Hydrogen H ₂ ^b	7.8 × 10 ⁻⁴
Denitrification	CH ₂ O + 0.8NO ₃₋ + 0.8H ⁺ → CO ₂ + 0.4N ₂ + 0.35H ₂ O	Nitrogen N ₂ ^b	6.5 × 10 ⁻⁴
Methanogenesis	CH ₂ O → 0.5CH ₄ + 0.5CO ₂	Methane CH ₄ ^b	1.4 × 10 ⁻³

^aFrom (Wilhelm et al. 1977).

^bBeside CO₂.

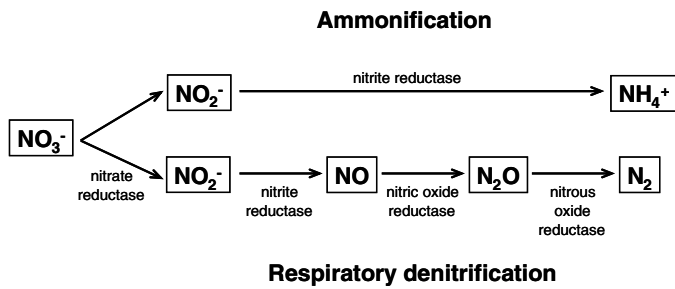


Fig. 1. Nitrate and nitrite reduction—enzymes involved

Denitrification does not always reach the last step of N_2 formation with 100% efficiency (lower branch in Fig. 1); hence, the produced gas is a combination of N_2O and N_2 at variable ratios (Barnes et al. 1995; Chung and Chung 2000; Davidson et al. 1993; Firestone et al. 1980; Johns et al. 2004). The most relevant factors influencing the ratio N_2O/N_2 include the presence of specific genes encoding the required enzymes in the bacterial species involved in the process; the ratio C/N (Chung and Chung 2000); the soil acidity and aeration (Barnes et al. 1995; Firestone et al. 1980; Johns et al. 2004); the soil texture and nutrient status (Johns et al. 2004); and the soil moisture (Davidson et al. 1993). The reduction of N_2O to N_2 is more effective under alkaline conditions because the activity of denitrifiers is higher when the surrounding pH ranges from pH 6 to 8. In soils with very high moisture, N_2 can be a significant end-product of denitrification, whereas in relatively dry soils, N_2O production by denitrification is generally rare and N_2O becomes the dominant end-product (Davidson et al. 1993). Despite the obvious advantages of denitrification for the purposes of this study, the potential release of incomplete denitrification by-products to the atmosphere or groundwater needs to be addressed in detail before attempting to apply this methodology in the field.

Gas Bubble Nucleation

Biogenic gases dissolve in the pore fluid (i.e., gas molecules occupy cavities between water molecules) until the fluid reaches the supersaturation threshold that prompts bubble nucleation (Ronen et al. 1989). Spontaneous bubble nucleation can result from (1) depressurization to a vapor pressure below that of the pure liquid; (2) temperature increase until the vapor becomes more stable than the pure liquid; or (3) dissolution of gas from a supersaturated liquid when the supersaturation exceeds certain threshold values (Hemmingsen 1975, 1977; Lubetkin 2003).

Supersaturation thresholds for homogeneous nucleation in the bulk liquid are a function of molecular interactions between the liquid and the dissolved gas; however, the presence of mineral surfaces tends to favor heterogeneous bubble nucleation at substantially lower supersaturations (Blander 1979; Gerth and Hemmingsen 1980; Pease and Blinks 1947). Nucleation centers in porous media include microcavities, irregularities, and impurities at mineral surfaces (Dominguez et al. 2000).

Once supersaturation is reached, the pore water pressure u approaches the pressure in the gas p_g (partial pressure when a single gas species is taken into account), and bubbles form unless the pressure in the fluid increases. The concentration of gas in the aqueous phase c_a is related to the gas pressure through Henry's constant k_H , as expressed in Henry's Law:

$$k_H = \frac{c_a}{p_g} \quad \text{Henry's Law} \quad (1)$$

Henry's constant depends on the gas species (see Table 2 for typical values). The tiny bubbles or "embryos" that form at bubble nucleation sites are stable only after reaching a critical size (Finkelstein and Tamir, 1985; La-Mer 1952; Ward et al. 1970). The critical radius r_{critical} is defined as (Lubetkin 2003)

$$r_{\text{critical}} = \frac{2 \cdot T_S}{\sigma \cdot u} \quad (2)$$

where T_S = the surface tension (~ 0.072 N/m for water at 20°C), σ = the supersaturation, and u = the pressure at which bubbles nucleate. Bubbles smaller than r_{critical} tend to redissolve into the pore fluid. On the other hand, stable bubbles $r > r_{\text{critical}}$ can migrate and/or coalesce to form larger bubbles that can eventually become trapped at pore throats defining Laplacian capillary surfaces (i.e., water-vapor interfaces that satisfy Laplace's equation). When Henry's Law applies, supersaturation is defined as

$$\sigma = \frac{c_{\text{gen}}}{c_{\text{eq}}} - 1 \quad (3)$$

where c_{gen} = the gas concentration in the fluid and c_{eq} = the gas concentration soluble in the liquid under the prevailing experimental conditions.

In most cases, theoretical arguments predict much higher supersaturations than experimentally found (Lubetkin 2003). These differences necessitate the use of macroscopic values for surface tension to analyze very small clusters representing subcritical and critical nuclei (Lubetkin 2003). They indicate the reduction of free energy needed to create a critical bubble nucleus due to geometrical imperfections (Wilt 1986); the existence of "active sites" on a heterogeneous surface that can be chemically, structurally, or geometrically inhomogeneous and therefore more catalytic than others surfaces (Deutscher and Fletcher, 1990; Kozisek et al. 2000); inhomogeneous supersaturation away from thermodynamic equilibrium (Li and Yortsos 1994); and secondary nucleation, whereby pre-existing bubbles behave as nucleation centers for new bubbles (Bergman and Mesler 1981).

A compilation of experimentally determined supersaturation values for different gases is presented in Table 3 (Lubetkin 2003). These values, combined with Eq. (2), can be used to estimate the range of critical sizes of bubble nuclei for specific gas species. Fig. 2 shows the range of critical sizes of bubble nuclei for nitrogen gas. The supersaturation range shown in Fig. 2 corresponds to that observed experimentally in Lubetkin (2003) (Table 3). The bubble nucleation pressure for experiments in this study can be considered equal to atmospheric pressure (~ 100 kPa, the thickest line in the plot).

Table 3. Measured Values of Supersaturation Needed to Cause Bubble Nucleation in Aqueous Solutions

Gas	Measured supersaturation needed
Carbon dioxide CO_2	4.62–20
Hydrogen H_2	80–90
Nitrogen N_2	19–140
Methane CH_4	80

Note: supersaturation is defined as: $\sigma = (c_{\text{gen}}/c_{\text{peq}}) - 1$, where c_{gen} is the gas concentration in the fluid, c_{eq} is the gas concentration soluble in the liquid under the experimental conditions used; compiled from Lubetkin (2003).

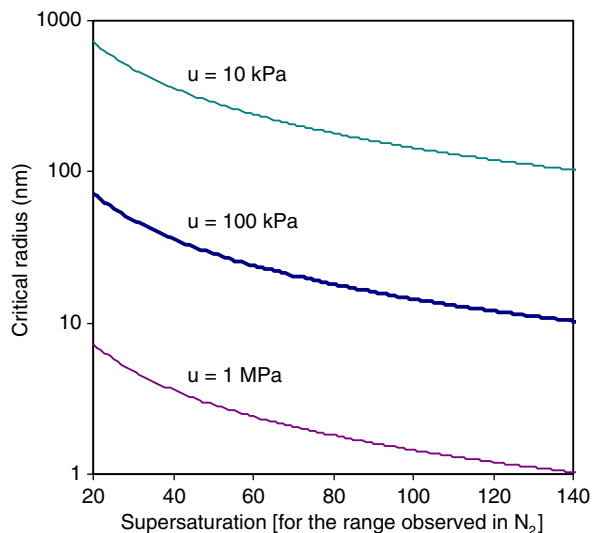


Fig. 2. Critical radius for N_2 bubble nucleation under different bubble nucleation pressures and supersaturation values, calculated using Eq. (2)

Experimental Study

This experimental study aimed to evaluate the ability of *Paracoccus denitrificans* to generate gas inside different soil types, to monitor gas bubble nucleation inside the soil matrix, and to assess the evolution of P -wave velocity in time. Additionally, the effects of nutrient availability and fines content on gas generation and P -wave velocity were also explored. The study was limited to low-confinement, and most tests were conducted under no nutrient-recharge conditions.

Materials and Devices

Sediments. Seven sediments were chosen for their particle size and compatible solution pH: Ottawa 20–30 sand (Ottawa, $d_{10} = 0.5$ mm, $d_{50} = 0.72$ mm, $C_u = 1.15$), F110 sand (F110, $d_{10} = 90$ μ m, $d_{50} = 0.12$ mm, $C_u = 1.62$), crushed silica flour (Sil-co-sil, $d_{10} = 10$ μ m, $S_a = 0.113$ m²/g), precipitated silica flour (Zeo, $d_{10} = 20$ μ m, $S_a = 6$ m²/g), RP2 kaolinite (RP2, $d_{10} = 0.36$ μ m, $S_a = 33$ m²/g Wilkinson), SA1 kaolinite (SA1, $d_{10} = 0.4$ μ m, $S_a = 36$ m²/g Wilkinson) and montmorillonite (Bent, $d_{10} = 0.0034$ μ m, $S_a = 200$ m²/g). Grain-size information was obtained following ASTM D 422, and the specific surface S_a

was measured using methylene blue (Santamarina et al. 2002). In addition, clayey-sand mixtures were prepared by combining these sediments.

Bacterial species. The selected strain is *Paracoccus denitrificans* (ATCC 13543), a nonmotile coccoid soil organism from the alpha subdivision of the proteobacteria. It is able to reduce nitrate to dinitrogen under anaerobic growth conditions (denitrification—Fig. 1). The four oxido-reductases required for the denitrification pathway (Mohan et al. 2004; Moura and Moura, 2001; Richardson et al. 2001; Simon 2002), along with their corresponding structural, accessory, and regulatory genes, have been well characterized in *P. denitrificans* [Baker et al. 1998].

Cells were grown in solid agar plates (Nutrient agar, Difco—Fisher Scientific) and incubated at their optimum temperature. Culture broth (Nutrient broth, Difco—Fisher Scientific) vials were inoculated with fresh colonies, grown for several days until reaching the late exponential phase [as verified in a previous study (Rabata-Landa 2007), results not shown], harvested, washed in saline solution and resuspended in a different culture broth (Nitrate broth Difco—Fisher Scientific) to enhance their denitrification potential. Previous studies using *P. denitrificans* and nitrate-rich broth corroborate the generation of nitrogen gas (*P. Sobecky*, personal communication, October 2006). The resuspended mixture will be referred to as the “bacterial inoculum.” In all tests, cells were resuspended immediately before specimen assemblage to prevent cell aging and deterioration.

Devices. The system consisted of a set of square Nalgene bottles, embraced by a rigid frame and sealed using rubber stoppers with two exit ports (Fig. 3). A capillary tube fitted through one port was used to determine the volume of produced gas. The other port was used to expel excess air during the specimen assemblage, and it was shut off after assemblage, (except in tests when it was used to inject additional nutrient at different time intervals).

P -wave velocity measurements across the specimens were performed using a set of piezocrystals (50 mm in diameter, resonance frequency of 50 kHz), that were externally coupled to the Nalgene bottles. The standard peripheral electronics used involved a pulse generator, amplifier, analog filter, and oscilloscope.

Test Procedure

Specimen preparation. All materials and equipment in contact with the bacterial inoculum (broths, agar, soils, water, capillary tubes, rubber stoppers, and bottles) were sterilized using a steam autoclave at 124°C and 125 kPa for 35 min prior to assemblage. All assemblage processes were conducted under aseptic conditions.

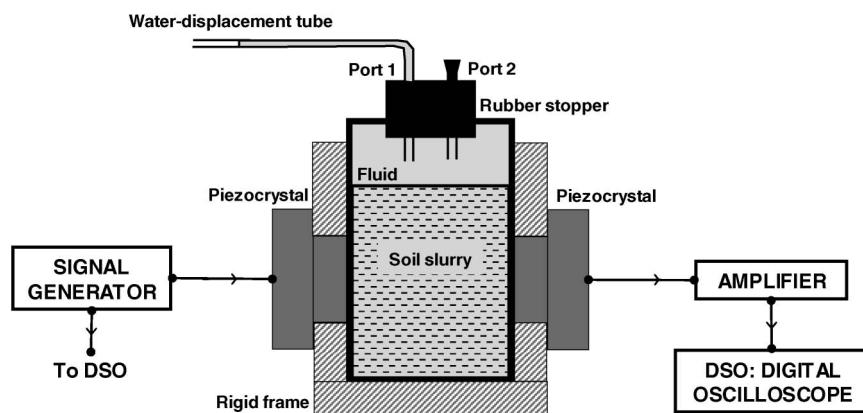


Fig. 3. Experimental device and peripheral electronics

Table 4. Tested Specimens—Preparation

Study	Soil	Soil (g) ^a	Inoculum (mL)	Nutrient (mL)	Water (mL)
Study #1 and #2	Bent	49.7	10	200	200
	SA1	227.08	10	200	200
	RP2	223.67	10	200	200
	Zeo	66.01	10	200	200
	Sil	575.67	10	200	50
	F110 (1st trial)	637.21	10	200	0
Study #3	F110 (2nd trial)	640	10	200	0
	Ottawa	728.58	10	200	0
	Sil (A)	576	10	200	50
Study #4	Sil (B)	576	10	200	50
	F110 + 1% Bent	646.4	10	200	0
	F110 + 3% Bent	618	10	200	0
	F110 + 9% Bent	327	10	200	0
	F110 + 10% Bent	363	10	200	50
	F110 + 15% Bent	281.8	10	200	50
	F110 + 3% RP2	618	10	200	0
	F110 + 9% RP2	545	10	200	0
F110 + 15% RP2	575	10	200	0	

^aTotal soil weight; mixtures are reported in percentage by weight.

Soil slurries were prepared by mixing specific amounts of each soil (or mixture), bacterial inoculum, and fresh nitrate broth, as indicated in Table 4. Slurries were poured into individual Nalgene bottles, subjected to vacuum to ensure initial saturation, and filled to the top with deionized, sterile, and deaired water. Rubber stoppers were set in place along with the water-displacement capillary tube. Initial assessments of *P*-wave velocity were made; when the initial *P*-wave velocity values were lower than ~1,400 m/s, additional vacuum was applied to remove any remaining gas to ensure that the initial soil saturation was $S \approx 100\%$.

Measurements. The *P*-wave velocity and the volume of produced gas (water displaced in the capillary tube) were recorded daily for a period of one month for all specimens. On day 30, some of the specimens were subjected to a step increase in pore fluid pressure of 20 kPa for 12 to 24 h to monitor the partial recovery of *P*-wave velocity.

Study #1: Sterile control. A parallel set of all seven soils was tested during 30 days using heat-killed bacteria instead of vegetative cells to verify that gas bubbles did not form and that the *P*-wave velocity remained constant under abiotic conditions.

Study #2: Single-grained soils. The selected soils were tested with nutrient added only at time zero. All seven specimens were subjected to the additional pore fluid pressure step increase after 30 days.

Study #3: Nutrient availability effect. Two additional bottles containing Sil-co-sil were used to study the influence of nutrient availability on *P*-wave velocity and generated gas evolution. Initial conditions were identical to those in Study #2. After the first measurement, one bottle (A) was injected with 1 mL of fresh Nitrate broth daily; the other bottle (B) was injected again 10 and 20 days after assemblage with 10 mL of fresh Nitrate broth each time.

Study #4: Mixed soils—Effects of fines content. Eight bottles containing F110 sand with different amounts and types of fines were tested to explore the role of mineral surfaces and gas entrapment. Bottle A contained only F110 sand, bottles B, C, D, and E contained 3, 9, 10, and 15% bentonite, respectively, and bottles F, G, and H contained 3, 9, and 15% RP2 kaolinite, respectively.

Bottles C and G (containing 9% bentonite and 9% RP2 kaolinite, respectively) were also used for the pore fluid pressure step test.

The complete data set and results for these studies can be found in Rebata-Landa (2007). Specific results and observations follow.

Results and Observations

Typical sets of *P*-wave signatures are presented in Fig. 4 for F110 sand mixed with different percentages of RP2 kaolinite. (The first signal in each sequence was gathered immediately after the initiation of the test. Successive signals were captured every day thereafter.) Similar *P*-wave signature results were observed when F110 sand was mixed with bentonite. Fig. 5 shows the evolution of *P*-wave velocity and generated gas volume versus time for F110 sand mixed with different percentages of bentonite. Analogous *P*-wave velocity results were observed when F110 sand was mixed with RP2 kaolinite. Once again, parallel measurements were gathered for all specimens. These results suggest a strong correlation between biogas volume generation and *P*-wave velocity evolution.

In all sterile controls, the *P*-wave velocity remained unchanged and no gas was generated (Study #1—data not shown); therefore, it is assumed that all changes observed in Figs. 4 and 5 are attributable to the biogenic gas generation inside the sediment.

In Fig. 6, the initial ($t \sim 0$) and final ($t \sim 30$ days) values of *P*-wave velocity for all specimens are plotted versus specific surface. In the figure, the arrow (data for Sil-co-sil) shows the effect of nutrient injections on final *P*-wave velocity. Original specimens appear as a solid diamond. The two specimens that received nutrient injections daily and every 10 days are shown as an asterisk and a dash, respectively. In all cases, *P*-wave velocity seems to stabilize around $V_p = 500\text{--}600$ m/s. Results summarized in Fig. 6 also indicate that *P*-wave velocity can be further modified by consecutive nutrient injections (Study #3): the *P*-wave velocity in crushed silica decreased to 682 m/s in the standard test (gas generation: 1 ml after 30 days), to 535 m/s with daily nutrient addition (gas generation: 2 ml after 30 days), and to 583 m/s when nutrient was added on the 10th and 20th days (gas generation: 1.4 ml after 30 days). Therefore, the minimum *P*-wave velocity measured in this study is not necessarily a boundary imposed by the system, but a limitation due to nutrient exhaustion, and for this reason nutrient availability could be used as a tool to control the extent of biogas generation in the soil.

Figs. 4 and 5 show that changes in *P*-wave velocity and gas generation are triggered earlier in specimens with higher fines content (Studies #2 and #4). When the percentage of fines is lower than 9% (both kaolinite and bentonite), abrupt changes in *P*-wave velocity and generated gas volume are followed by a partial recovery, and finally reach a stable value. This transient is not observed in soils with higher fines content.

Pore fluid pressure step. The time-dependent increase in *P*-wave velocity for the nine tested specimens is plotted in Fig. 7. The pressure was increased from the initial value equal to the atmospheric pressure to a constant value of $u = 20$ kPa above the atmospheric pressure. Although the 20 kPa increase in pore fluid pressure is applied almost instantaneously, it takes about 15 h for the *P*-wave velocity to stabilize.

Dismantling specimens. All bottles were sealed and vigorously shaken by hand before disposal. Gas bubbles coalesced and formed larger bubbles that could be seen by the naked eye and raised toward the surface. Specimens with high fines content required significantly more shaking than those with low fines content to release the gas, clearly showing the role of fines in gas entrapment.

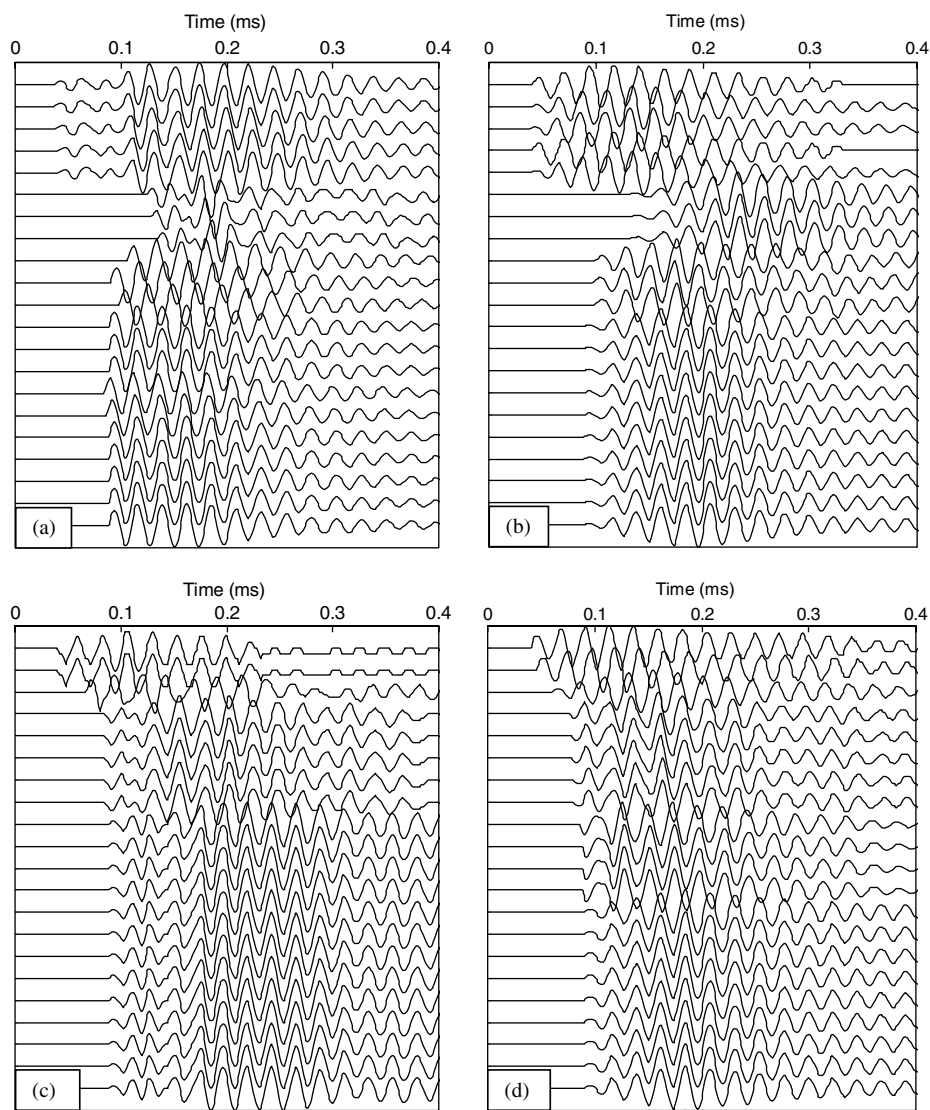


Fig. 4. Evolution of P -wave signatures during biogenic gas formation: (a) F110 sand without fines; (b) F110 + 3%RP2; (c) F110 + 9%RP2; (d) F110 + 15%RP2.

Analysis and Discussion

Effect of Fines Content

No transient was observed in the P -wave velocity versus time data (Fig. 4) for soils with some fines content. Apparently, fines hinder the motion of gas bubbles, trapping them in the soil matrix. Conversely, bubbles can escape in the absence of fines and the P -wave velocity partially recovers, causing the observed transient in the data.

The maximum volume of generated gas is plotted versus specific surface in Fig. 8. The strong correlation observed for all tested sediments is directly linked to the availability of nucleation sites on mineral surfaces (i.e., heterogeneous nucleation), which in turn, also affects the degree of attainable supersaturation.

Gas Bubbles and Bulk Stiffness—Bubble Size

Bubbles much smaller than soil particles can fit within the pore space without distorting the soil structure; thus, the presence of gas bubbles only changes the compressibility of the pore fluid (Wheeler 1988). Even relatively small size bubbles are sufficient

to significantly change the pore fluid bulk stiffness (Sparks 1963). The pore fluid bulk stiffness κ_f depends on the degree of saturation S , the bulk stiffness of water κ_w (~ 2.2 GPa), and the bulk stiffness of gas bubbles κ_b . Relevant mixture formulas are summarized in Table 5.

The bulk stiffness of bubbles can be estimated by defining bulk stiffness as

$$\kappa_b = \left| \frac{\partial P}{\partial V/V_0} \right| \quad (4)$$

where the volume V of a bubble is a function of its radius r :

$$V = \frac{4}{3} \cdot \pi \cdot r^3 \quad (5)$$

The following assumptions are made: (1) the bubbles are isolated, (2) there is a continuous water phase, and (3) the vapor-water interface is not in contact with the mineral surfaces. Under these conditions, the gas pressure inside the bubble P is related to the pressure in the surrounding water u_w and the surface tension T_s , according to Laplace's equation:

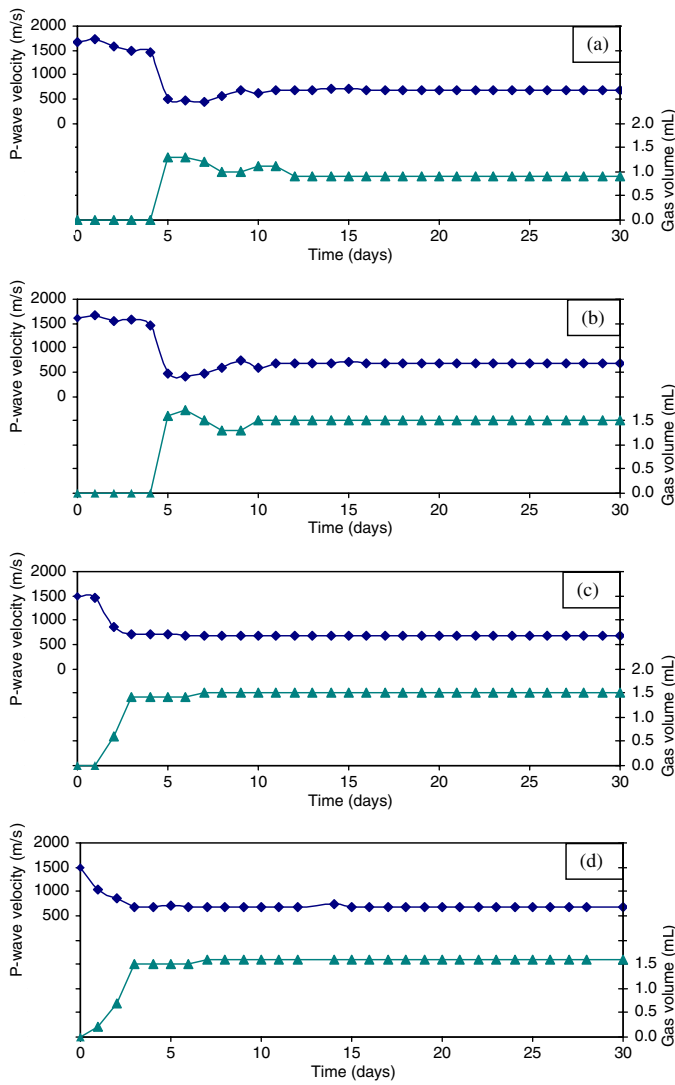


Fig. 5. *P*-wave velocity and generated gas data for (a) F110 sand without fines; (b) F110 + 3% bentonite; (c) F110 + 9% bentonite; (d) F110 + 15% bentonite

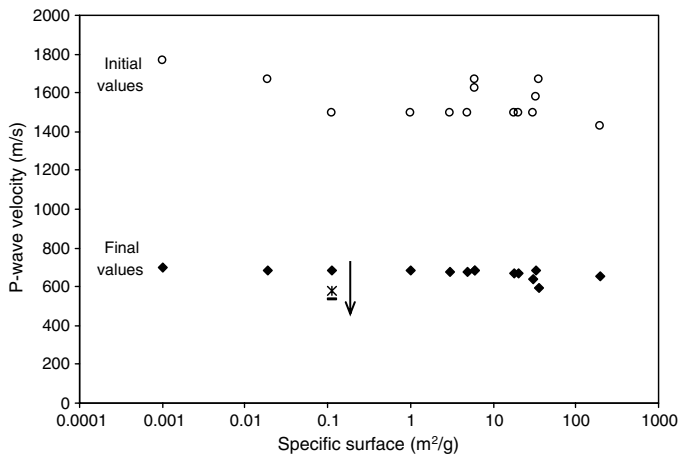


Fig. 6. Initial ($t = 0$) and final ($t = 30$ days) steady-state *P*-wave velocity for all specimens, both single-grained soils and mixtures, as a function of the specific surface.

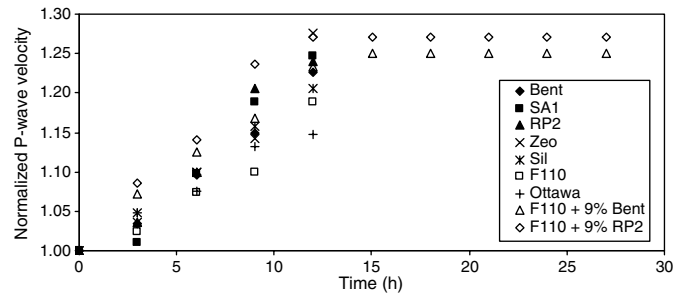


Fig. 7. *P*-wave velocity recovery as a function of time after the step increase in the pore fluid pressure.

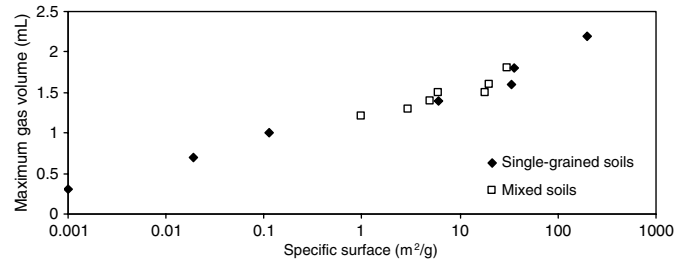


Fig. 8. Maximum volume of generated gas versus specific surface versus (30 days); for clarity, the cases with additional nutrient are not included

Table 5. Bulk Stiffness, Mass Density and Propagation Velocity [Adapted from Santamarina et al. (2001)]

Parameter	Equation
(a) Fluid bulk stiffness	$\kappa_f = \frac{1}{\frac{n}{\kappa_w} + \frac{1-n}{\kappa_b}}$
(b) Bulk stiffness of a soil suspension	$\kappa_{sus} = \frac{1}{\frac{n}{\kappa_f} + \frac{1-n}{\kappa_g}}$
(c) Bulk stiffness of a fluid-filled soil ^a	$\kappa_{soil} = \kappa_{sk} + \kappa_{sus} = \kappa_{sk} + \frac{1}{\frac{n}{\kappa_f} + \frac{1-n}{\kappa_g}}$
(d) Mass density	$\rho_{soil} = (1 - n) \cdot \rho_g + n \cdot S \cdot \rho_w$
(e) <i>P</i> -wave velocity	$V_P = \sqrt{\frac{\kappa_{soil} + \frac{4}{3}G_{soil}}{\rho_{soil}}}$
(f) <i>S</i> -wave velocity	$V_S = \sqrt{\frac{G_{soil}}{\rho_{soil}}}$

Note: where n = the porosity; S = the degree of saturation, κ_{soil} , κ_{sk} , κ_{sus} , κ_g , κ_f , κ_w and κ_b = the bulk stiffness of the mixture, the soil skeleton, the soil suspension, the soil particle (material that forms the grains ~ 37 GPa), the pore fluid, the water (~ 2.2 GPa), and the gas bubbles, respectively; V_P and V_S = the *P*-wave and *S*-wave velocity, respectively; G_{soil} = the shear stiffness of the soil mass, and ρ_{soil} = the mass density of the soil mass.

^aApplicable to near-surface soils at low-confinement, where $\kappa_g \gg \kappa_{sk}$; otherwise, the Gassmann equation must be used instead.

$$P = u_w + \frac{2 \cdot T_s}{r} \quad (6)$$

Therefore, the bubble bulk stiffness is

$$\kappa_b = \frac{2 \cdot T_s}{3 \cdot r} \quad (7)$$

Combining Equation (a) from Table 5 and Eq. (7), the fluid bulk stiffness becomes:

$$\kappa_f = \frac{1}{S \frac{1}{\kappa_w} + (1 - S) \frac{3 \cdot r}{2 \cdot T_s}} \quad (8)$$

In contrast, the bulk modulus of a suspension of mineral particles in a fluid κ_{sus} takes into account the volumetric changes in grains attributable to changes in pore fluid pressure, as indicated in Equation (b) in Table 5. In addition, when particles come into contact with each other, the granular skeleton shares the load with the fluid, resulting in Equation (c) in Table 5. These equations can be sequentially combined to obtain a general expression for the bulk stiffness of sediments in the presence of disseminated gas bubbles:

$$\kappa_{\text{soil}} = \kappa_{sk} + \frac{1}{n[S\frac{1}{\kappa_w} + (1-S)\frac{3r}{2T_s}] + \frac{1-n}{\kappa_g}} \quad (9)$$

In laboratory and field applications, the global bulk stiffness of the soil κ_{soil} and its skeletal stiffness κ_{sk} can be inferred from P - and S - wave velocity measurements, as indicated in Table 5. Then, these expressions permit estimating the average bubble radius as a function of P - and S -wave velocity and degree of saturation (for $S < 1$):

$$r = \frac{2 \cdot T_s}{3 \cdot (1 - S)} \cdot \left(\frac{1}{n} \left\{ \frac{1}{\rho_{\text{soil}}[V_p^2 - (\frac{4}{3} + \alpha) \cdot V_s^2]} - \frac{1 - n}{\kappa_g} \right\} - \frac{S}{\kappa_w} \right) \quad (10)$$

where α depends on the Poisson's ratio of the skeleton ν_{sk} and varies between $\alpha = 0.92$ -to- 1.33 for $\nu_{sk} = 0.1$ -to- 0.2 , respectively.

The evolution in average bubble radius was estimated for each experiment using this expression. Maximum values of average bubble radius ranged from 28 nm to 350 nm. These sizes are larger than the critical radius $r_{\text{critical}} = 10$ nm computed for the prevailing experimental conditions (atmospheric pressure, nitrogen gas—Fig. 2); therefore, they are stable bubbles. No explicit correlation is found between the average bubble radius and the specific surface of the various sediments.

Skempton's B -Value and P -Wave Velocity

Skempton's B -value is the ratio of the change in pore fluid pressure Δu for a change in isotropic confinement $\Delta \sigma$ applied under undrained conditions (Skempton 1954):

$$B = \frac{\Delta u}{\Delta \sigma} \quad (11)$$

From poroelasticity, the parameter B can be expressed as a function of the bulk stiffness of the mineral that makes the grains κ_g , the granular skeleton κ_{sk} , and the whole soil mass κ_{soil} (Ishihara 1970):

$$B = \frac{1 - \frac{\kappa_{sk}}{\kappa_{\text{soil}}}}{1 - \frac{\kappa_{sk}}{\kappa_g}} \approx 1 - \frac{\alpha}{\left(\frac{V_p}{V_s}\right)^2 - \frac{4}{3}} \quad (12)$$

where the approximation applies for $\kappa_{sk}/\kappa_g \rightarrow 0$. Replacing Eq. (9) in (12), an alternative asymptotic solution for B when $\kappa_{sk}/\kappa_g \rightarrow 0$ is (Skempton 1954):

$$B = \frac{1}{1 + n \cdot \frac{\kappa_{sk}}{\kappa_f}} \quad (13)$$

A convenient expression for Skempton's B parameter can be derived by substituting equations in Table 5, Eq. (8) and (10) in Eq. (13):

$$B = \frac{1}{1 + \alpha \cdot \rho_{\text{soil}} \cdot V_s^2 \left\{ \frac{1}{\rho_{\text{soil}}[V_p^2 - (\frac{4}{3} + \alpha) \cdot V_s^2]} - \frac{1 - n}{\kappa_g} \right\}} \quad (14)$$

Whereas the S -wave velocity in granular media is determined by the skeletal stiffness and it remains practically unchanged during

the early stages of unsaturation [i.e., κ_{sk} is not affected at low suction (Cho and Santamarina 2001)], the P -wave velocity is controlled by the bulk stiffness of the pore fluid and it rapidly decreases as soon as $S < 1$ (Ishihara et al. 1998; Tsukamoto et al. 2002). Hence, V_p is significantly larger than V_s near saturation. Computed $B - V_p$ trends are plotted together with published experimental data in Fig. 9. The experimental data in this figure is collected from the literature identified. The lines correspond to Eq. (12) for $\alpha = 2.0$ and two different shear wave velocities V_s .

Effect of Biogenic Gas on Liquefaction Resistance

The number of cycles required to attain liquefaction considerably increases as the value of B decreases (Ishihara et al. 1998; Sherif et al. 1977; Tsukamoto et al. 2002; Yang 2002; Yoshimi et al. 1989). Published results are summarized in Fig. 10 (right). From the point of view of field applications, a correlation between V_p and the cyclic stress ratio is particularly convenient. This correlation is supported by the causal link between saturation, and fluid bulk stiffness interacting with both B -value and P -wave velocity, as shown above. This relationship is explored in Fig. 10 (left), using published results (data collected from the literature identified in the figure). It can be concluded that the cyclic stress ratio increases by about 20% when the P -wave velocity decreases from $V_p = 1500$ m/s to $V_p = 600$ m/s, and exhibits a dramatic improvement when the P -wave velocity drops below $V_p \sim 500$ m/s. These

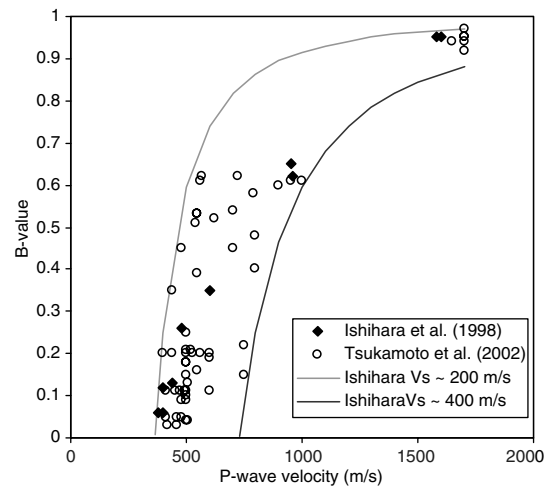


Fig. 9. Relationship between B -value and P -wave velocity

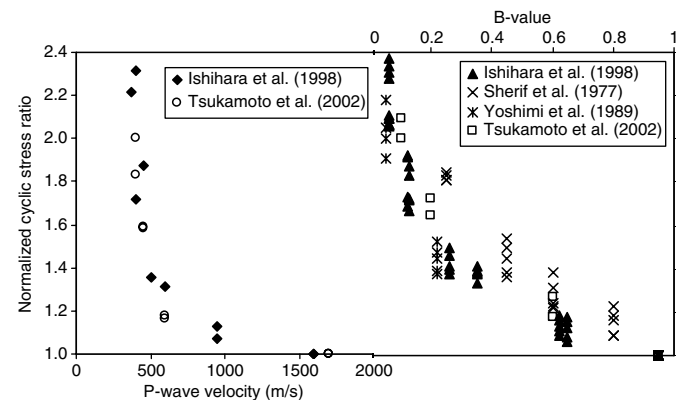


Fig. 10. Variation in normalized cyclic stress ratio (NCSS) with respect to P -wave velocity (left) and B -value (right)

observations, in combination with the results shown in Figs. 5 and 6, suggest the potential use of biogenic gas generation (nitrogen gas in this study) to increase the liquefaction resistance of soils subjected to cyclic loading.

Effect of Pore Fluid Pressure Fluctuations in Bubble Dissolution

The results from the pore fluid pressure step tests (Fig. 7) reflect time-dependent bubble dissolution. In other words, gas bubbles compress as the fluid pressure is increased, and later experience diffusion-limited dissolution to reach the new equilibrium condition. This phenomenon may be relevant to tidal or water surge events as they impose a fluid pressurization transient.

Conclusions

Biogenic gas generation (nitrogen gas in this study) effectively reduces the bulk stiffness of the pore fluid, the P -wave velocity, Skempton's B parameter (relative to the soil shear stiffness), and the susceptibility to liquefaction.

Biogenic gas generation is temperature dependent because of the inherent nature of bacterial growth dynamics. Controlled nutrient injection can be used to regulate the process. Ultimately, the type, quantity, and rate of biogenic gas production may be "designed" to address specific engineering needs.

There was no response in any of the sterile controls. In contrast, consistent changes in P -wave velocity and gas volume were observed in inoculated sediments. This suggests that, the generated gas is biomediated and cannot be explained by chemical effects associated with the addition of nutrients to the soil.

Biogenic gas forms submicron-size bubbles which are disseminated throughout the soil mass; this pattern contrasts with that of air injection, which tends to concentrate along percolation paths. Thus, the biogenic gas alternative may be more effective at preventing the local triggering of liquefaction. This hypothesis needs further evaluation.

Soil grain size affects the early evolution of bio-mediated gas generation by contributing nucleation sites as well as entrapment. Sands with small percentages of fines may fail to trap bubbles and may show a transient decrease in P -wave velocity, followed by a partial recovery to the final stable value. When the fines content increases, the transient does not take place, and sands reach a stable P -wave velocity faster than in clean sands.

Bacteria and nutrients must be properly selected so that the generated gases are environmentally safe, have low solubility in water, facilitate bubble formation, and experience relatively long residency time. Although nitrogen gas appears to exhibit all these characteristics, possible by-products in an incomplete denitrification pathway are environmentally inadequate and should be further analyzed.

P -wave propagation provides insightful information that can be effectively used to monitor biogenic gas generation in laboratory applications. Furthermore, this geophysical method is readily applicable in the field. Pore fluid pressure step experiments and theoretical arguments suggest that biogas generation effects will require longer time under higher pore fluid pressure conditions in the field.

Acknowledgments

Support for this research was provided by the National Science Foundation and The Goizueta Foundation.

References

- Adams, D. D., Fendiger, N. J., and Glotfelty, D. E. (1990). "Biogenic gas production and mobilization of in-place sediment contaminants by gas ebullition." *Sediments: Chemistry and toxicity of in-place pollutants*, R. Baudo, J. Giesy, and H. Muntau, eds., CRC Press, Boca Raton, FL, 215–236.
- Baker, S. C., Ferguson, S. J., Ludwig, B., Page, M. D., Richter, O. M. H., and van Spanning, R. J. M. (1998). "Molecular genetics of the genus *Paracoccus*: Metabolically versatile bacteria with bioenergetic flexibility." *Microbiol. Mol. Biol. Rev.*, 62(4), 1046–1078.
- Barnes, J. M., Apel, W. A., and Barrett, K. B. (1995). "Removal of nitrogen oxides from gas streams using biofiltration." *J. Hazard. Mater.*, 41(2–3), 315–326.
- Behlulgi, K., and Mehmetoglu, M. T. (2002). "Bacteria for improvement of oil recovery: A laboratory study." *Energy Sources*, 24(5), 413–421.
- Bergman, T., and Mesler, R. (1981). "Bubble nucleation studies. 1.- Formation of bubble nuclei in superheated water by bursting bubbles." *AIChE J.*, 27(5), 851–853.
- Blander, M. (1979). "Bubble nucleation in liquids." *Adv. Colloid Interface Sci.*, 10(1), 1–32.
- Buttler, A. J., Dinel, H., Levesque, M., and Mathur, S. P. (1991). "The relation between movement of subsurface water and gaseous methane in a basin bog with a novel instrument." *Can. J. Soil Sci.*, 71(4), 427–438.
- Cannavo, P., Richaume, A., and Lafolie, F. (2004). "Fate of nitrogen and carbon in the vadose zone: In situ and laboratory measurements of seasonal variations in aerobic respiratory and denitrifying activities." *Soil Biol. Biochem.*, 36(3), 463–478.
- Cardenas, L. M., Hawkins, J. M. B., Chadwick, D., and Scholefield, D. (2003). "Biogenic gas emissions from soils measured using a new automated laboratory incubation system." *Soil Biol. Biochem.*, 35(6), 867–870.
- Chaney, R. C. (1978). "Saturation effects on the cyclic strength of sands." *Proc., Specialty Conf. on Earthquake Engineering and Soil Dynamics*, ASCE, Reston, VA, Vol. 1, 342–358.
- Cho, G. C., and Santamarina, J. C. (2001). "Unsaturated particulate materials—Particle-level studies." *J. Geotech. Geoenviron. Eng.*, 127(1), 84–96.
- Chung, Y. C., and Chung, M. S. (2000). "BNP test to evaluate the influence of C/N ratio on N_2O production in biological denitrification." *Water Sci. Technol.*, 42(3–4), 23–27.
- Cole, J. A., and Brown, C. M. (1980). "Nitrite reduction to ammonia by fermentative bacteria: A short circuit in the biological nitrogen-cycle." *FEMS Microbiol. Lett.*, 7(2), 65–72.
- Constantz, J., Herkelrath, W. N., and Murphy, F. (1988). "Air encapsulation during infiltration." *Soil Sci. Soc. Am. J.*, 52(1), 10–16.
- Daniels, L., Fulton, G., Spencer, R. W., and Orme-Johnson, W. H. (1980). "Origin of hydrogen in methane produced by *Methanobacterium thermoautotrophicum*." *J. Bacteriol.*, 141(2), 694–698.
- Davidson, E. A., et al. (1993). "Processes regulating soil emissions of NO and N_2O in a seasonally dry tropical forest." *Ecology*, 74(1), 130–139.
- Deutscher, R. L., and Fletcher, S. (1990). "Nucleation on active sites. 5.- The theory of nucleation rate dispersion." *J. Electroanal. Chem.*, 277(1–2), 1–18.
- Dinel, H., Mathur, S. P., Brown, A., and Levesque, M. (1988). "A field study of the effect of depth on methane production in peatland waters: Equipment and preliminary results." *J. Ecol.*, 76(4), 1083–1091.
- Dominguez, A., Bories, S., and Pratt, M. (2000). "Gas cluster growth by solute diffusion in porous media. Experiments and automaton simulation on pore network." *Int. J. Multiphase Flow*, 26(12), 1951–1979.
- Fayer, M. J., and Hillel, D. (1986). "Air encapsulation. 1. Measurement in a field soil." *Soil Sci. Soc. Am. J.*, 50(3), 568–572.
- Finkelstein, Y., and Tamir, A. (1985). "Formation of gas bubbles in super-saturated solutions of gases in water." *AIChE J.*, 31(9), 1409–1419.
- Firestone, M. K., Firestone, R. B., and Tiedje, J. M. (1980). "Nitrous oxide from soil denitrification: Factors controlling its biological production." *Science*, 208(4445), 749–751.
- Forsythe, S. J., Dolby, J. M., Webster, A. D. B., and Cole, J. A. (1988). "Nitrate-reducing and nitrite-reducing bacteria in the achlorhydric stomach." *J. Med. Microbiol.*, 25(4), 253–259.

- Fourie, A. B., Hofmann, B. A., Mikula, R. J., Lord, E. R. F., and Robertson, P. K. (2001). "Partially saturated tailings sand below the phreatic surface." *Geotechnique*, 51(7), 577–585.
- Gallagher, P. M., and Mitchell, J. K. (2002). "Influence of colloidal silica grout on liquefaction potential and cyclic undrained behavior of loose sand." *Soil Dyn. Earthquake Eng.*, 22(9–12), 1017–1026.
- Gerth, W. A., and Hemmingsen, E. A. (1980). "Heterogeneous nucleation of bubbles at solid-surfaces in gas-supersaturated aqueous solutions." *J. Colloid Interface Sci.*, 74(1), 80–89.
- Hemmingsen, E. A. (1975). "Cavitation in gas-supersaturated solutions." *J. Appl. Phys.*, 46(1), 213–218.
- Hemmingsen, E. A. (1977). "Spontaneous formation of bubbles in gas-supersaturated water." *Nature*, 267(5607), 141–142.
- Ishihara, K. (1970). "Approximate forms of wave equations for water-saturated porous materials and related dynamic modulus." *Soils Found.*, 10(4), 10–38.
- Ishihara, K., Huang, Y., and Tsuchiya, H. (1998). "Liquefaction resistance of nearly saturated sand as correlated with longitudinal velocity." *Poromechanics—A tribute to Maurice, A. Biot, J. F. Thimus, Y. Abousleiman, A. H. D. Cheng, O. Coussy, and E. Detournay*, eds., Balkema, Rotterdam, Netherlands, 583–586.
- Ismail, M. A., Joer, H. A., Randolph, M. F., and Meritt, A. (2002). "Cementation of porous materials using calcite." *Geotechnique*, 52(5), 313–324.
- Johns, D., Williams, H., Farrish, K., and Wagner, S. (2004). "Denitrification and soil characteristics of wetlands created on two mine soils in east Texas, USA." *Wetlands*, 24(1), 57–67.
- Kokusho, T. (2000). "Correlation of pore-pressure B -value with P -wave velocity and poisson's ratio for imperfectly saturated sand or gravel." *Soils Found.*, 40(4), 95–102.
- Kozisek, Z., Demo, P., and Sato, K. (2000). "Nucleation on active sites: Evolution of size distribution." *J. Cryst. Growth*, 209(1), 198–202.
- La-Mer, V. K. (1952). "Nucleation in phase transitions." *Ind. Eng. Chem.*, 44(6), 1270–1277.
- Li, X., and Yortsos, Y. C. (1994). "Bubble growth and stability in an effective porous medium." *Phys. Fluids*, 6(5), 1663–1676.
- Logan, B. E., Oh, S. E., Kim, I. S., and van Ginkel, S. (2002). "Biological hydrogen production measured in batch anaerobic respirometers." *Environ. Sci. Technol.*, 36(11), 2530–2535.
- Lubetkin, S. D. (2003). "Why is it much easier to nucleate gas bubbles than theory predicts?" *Langmuir*, 19(7), 2575–2587.
- Martens, C. S., and Berner, R. A. (1974). "Methane production in interstitial waters of sulfate-depleted marine sediments." *Science*, 185(4157), 1167–1169.
- Mohan, S. B., Schmid, M., Jetten, M., and Cole, J. (2004). "Detection and widespread distribution of the *nrfA* gene encoding nitrite reduction to ammonia, a short circuit in the biological nitrogen cycle that competes with denitrification." *FEMS Microbiol. Ecol.*, 49(3), 433–443.
- Moura, I., and Moura, J. J. G. (2001). "Structural aspects of denitrifying enzymes." *Curr. Opin. Chem. Biol.*, 5(2), 168–175.
- Nakamura, M., Kanbe, H., and Matsumoto, J. I. (1993). "Fundamental studies on hydrogen production in the acid-forming phase and its bacteria in anaerobic treatment processes—The effects of solids retention time." *Water Sci. Technol.*, 28(7), 81–88.
- Pease, D. C., and Blinks, L. R. (1947). "Cavitation from solid surfaces in the absence of gas nuclei." *J. Phys. Colloid Chem.*, 51(2), 556–567.
- Rebata-Landa, V. (2007). "Biomediated phenomena in soil behavior." Ph.D. thesis, Georgia Institute of Technology, Atlanta, GA.
- Rebata-Landa, V., and Santamarina, J. C. (2006). "Mechanical limits to microbial activity in deep sediments." *Geochem. Geophys. Gesisyst.*, 7(Q11006), 12.10.1029/2006GC001355.
- Richardson, D. J., Berks, B. C., Russell, D. A., Spiro, S., and Taylor, C. J. (2001). "Functional, biochemical and genetic diversity of prokaryotic nitrate reductases." *Cell Mol. Life Sci.*, 58(2), 165–178.
- Ronen, D., Berkowitz, B., and Magaritz, M. (1989). "The development and influence of gas bubbles in phreatic aquifers under natural flow conditions." *Transp. Porous Media*, 4(3), 295–306.
- Santamarina, J. C., Klein, K. A., and Fam, M. A. (2001). *Soils and waves: [particulate materials behavior, characterization and process monitoring]*, Wiley, Chichester, UK.
- Santamarina, J. C., Klein, K. A., Wang, Y. H., and Prencke, E. (2002). "Specific surface: Determination and relevance." *Can. Geotech. J.*, 39(1), 233–241.
- Sherif, M. A., Ishibashi, I., and Tsuchiya, C. (1977). "Saturation effects on initial soil liquefaction." *J. Geotech. Eng. Div.*, 103(8), 914–917.
- Sills, G. C., and Gonzalez, R. (2001). "Consolidation of naturally gassy soft soil." *Geotechnique*, 51(7), 629–639.
- Sills, G. C., Wheeler, S. J., Thomas, S. D., and Gardner, T. N. (1991). "Behavior of offshore soils containing gas bubbles." *Geotechnique*, 41(2), 227–241.
- Simon, J. (2002). "Enzymology and bioenergetics of respiratory nitrite ammonification." *FEMS Microbiol. Rev.*, 26(3), 285–309.
- Skempton, A. W. (1954). "The pore-pressure coefficients A and B ." *Geotechnique*, 4(4), 143–147.
- Soares, M. I. M., Belkin, S., and Abeliovich, A. (1988). "Biological groundwater denitrification: Laboratory studies." *Water Sci. Technol.*, 20(3), 189–195.
- Sparks, A. D. W. (1963). "Theoretical considerations of stress equations for partly saturated soils." *Proc., 3rd African Conf. Soil Mech. Found. Eng.*, International Society for Soil Mechanics and Foundation Engineering, Vol. 1, 215–218.
- Tamura, S., Tokimatsu, K., Abe, A., and Sato, M. (2002). "Effects of air bubbles on B -value and P -wave velocity of a partly saturated sand." *Soils Found.*, 42(1), 121–129.
- Tiedje, J. M., Sextone, A. J., Myrold, D. D., and Robinson, J. A. (1982). "Denitrification: Ecological niches, competition and survival." *Antonie van Leeuwenhoek*, 48, 569–583.
- Tsukamoto, Y., Ishihara, K., Nakazawa, H., Kamada, K., and Huang, Y. N. (2002). "Resistance of partly saturated sand to liquefaction with reference to longitudinal and shear wave velocities." *Soils Found.*, 42(6), 93–104.
- Ward, C. A., Balakris, A., and Hooper, F. C. (1970). "On thermodynamics of nucleation in weak gas-liquid solutions." *J. Basic Eng.*, 92(4), 695–704.
- Wheeler, S. J. (1988). "A conceptual model for soils containing large gas bubbles." *Geotechnique*, 38(3), 389–397.
- Wilhelm, E., Battino, R., and Wilcock, R. J. (1977). "Low-pressure solubility of gases in liquid water." *Chem. Rev.*, 77(2), 219–262.
- Wilt, P. M. (1986). "Nucleation rates and bubble stability in water carbon dioxide solutions." *J. Colloid Interface Sci.*, 112(2), 530–538.
- Yang, J. (2002). "Liquefaction resistance of sand in relation to P -wave velocity." *Geotechnique*, 52(4), 295–298.
- Yang, J., Savidis, S., and Roemer, M. (2004). "Evaluating liquefaction strength of partially saturated sand." *J. Geotech. Geoenviron. Eng.*, 130(9), 975–979.
- Yegian, M. K., Eseller-Bayat, E., Alshawabkeh, A., and Ali, S. (2007). "Induced partial saturation for liquefaction mitigation: Experimental investigation." *J. Geotech. Geoenviron. Eng.*, 133(4), 372–380.
- Yoshimi, Y., Tanaka, K., and Tokimatsu, K. (1989). "Liquefaction resistance of a partially saturated sand." *Soils Found.*, 29(3), 157–162.